Low Probability of Intercept-Based Optimal Power Allocation Scheme for an Integrated Multistatic Radar and Communication System

Chenguang Shi , *Member, IEEE*, Fei Wang , Mathini Sellathurai, *Senior Member, IEEE*, Jianjiang Zhou, *Member, IEEE*, and Sana Salous , *Senior Member, IEEE*

Abstract—This paper investigates the problem of low probability of intercept-based optimal power allocation (LPI-OPA) for an integrated multistatic radar and communication system, which consists of multiple transmitters operating at different frequencies, a radar receiver, and a communication receiver (CR). The integrated multistatic radar and communication system is capable of fulfilling the requirements of both radar and communication subsystems. The key tenet of the integrated system is to minimize the total power consumption by optimizing the transmit power allocation at each transmitter for radar waveforms and information signals, which is constrained by a predetermined target detection performance for the RR and a desired information rate for the CR. Since the analytical closed-form expression of the probability of detection is not tractable, its upper bound is derived. We analytically show that the resulting optimization problem can be reformulated as two subproblems, which can be solved by an efficient solution procedure based on the approach of linear programming and the Karush–Kuhn–Tuckers optimality conditions. Simulation results are provided to show that the LPI performance of the integrated multistatic radar and communication system can significantly be enhanced by employing our proposed LPI-OPA scheme.

Index Terms—Information rate, integrated multistatic radar and communication system, low probability of intercept (LPI), optimal power allocation (PA), probability of detection.

C. Shi is with the Key Laboratory of Radar Imaging and Microwave Photonics, Ministry of Education and the Key Laboratory of Dynamic Cognitive System of Electromagnetic Spectrum Space, Ministry of Industry and Information Technology, Nanjing University of Aeronautics and Astronautics, Nanjing 210016, China (e-mail: scg_space@163.com).

F. Wang and J. Zhou are with the Key Laboratory of Radar Imaging and Microwave Photonics, Ministry of Education, Nanjing University of Aeronautics and Astronautics, Nanjing 210016, China (e-mail: wangxiaoxian@nuaa.edu.cn; zjjee@nuaa.edu.cn).

M. Sellathurai is with the School of Engineering and Physical Sciences, Herriot Watt University, EH14 4AS Edinburg, U.K. (e-mail: mathini@ieee.org).

S. Salous is with the School of Engineering and Computing Sciences, Durham University, DH1 3LE Durham, U.K. (e-mail: sana.salous@durham.ac.uk).

Digital Object Identifier 10.1109/JSYST.2019.2931754

I. INTRODUCTION

A. Background and Motivation

RECENTLY, the urgent need for faster communications and the rapid development of commercial multimedia applications have result in an increasing demand for radio frequency (RF) bandwidth [1]. The problem of spectral congestion has increasingly encouraged the radar band users to share RF bandwidth with a growing number of wireless communications devices [2]. As an emerging research topic, numerous studies investigating the coexistence of radar and wireless communications systems in the same frequency band have been proposed [3]–[11], which is able to minimize interference effects and ease the competition over spectrum bandwidth. In [1], Paul *et al.* perform a survey of previous RF communications and sensing convergence research, which provides a point of departure for future researchers to solve the underlying problem by presenting the topologies, levels of system integration, and the current technologies. In [3], the inner bounds on performance of radar and communications coexistence are defined and analytically derived. Similar work has been done in [4], in which several cooperative and codesign methods are proposed to provide improved spectral efficiency. Further, a cooperative strategy for the coexistence of a matrix completion based colocated multiple-input multiple-output (MIMO) radar and a MIMO communication system is developed in [5]. The main idea is to jointly optimize the radar transmit precoder, the radar subsampling strategy, and the communication transmit covariance matrix for a predetermined communication rate threshold, such that the radar signal-to-interference-plus-noise (SINR) ratio is maximized. Since multicarrier waveform is one of the best candidates for both radar and communication applications, the authors in [6]–[9] present the orthogonal frequency division multiplexing (OFDM) radar waveform optimization algorithms for spectrum sharing. As an extension, reference [10] formulates the power minimization-based robust OFDM radar waveform design for radar and communication systems in coexistence. Various waveform design schemes are proposed to minimize the worst-case power consumption of radar system by optimizing OFDM radar waveform subject to a certain mutual information (MI) requirement for target estimation and a minimum capacity for communication transferring. It is illustrated that the radar radiated power can be evidently reduced by employing the communication signals scattered off the target in radar system. In [11], the authors present a novel algorithm to enhance the spectrum sharing performance between MIMO radar and

downlink multiuser multiple-input single-output communication system.

In contrast to the above research, a more favorable idea is to design an integrated system that carries out both radar and communications. Traditionally, radar and wireless communications systems have been developed in isolation. Typically, the aim of a radar system is to detect and track enemy targets, while that of a communication system is to transfer information from a source to a sink [12]. Nevertheless, there are several similarities between the two RF functionalities, which makes the integrated design of radar and communication systems much more plausible. Technically speaking, this integrated radar and communication system can share the hardware and RF spectrum to achieve simultaneously both radar target detection and information transferring. In view of this, the integrated design not only reduces the size, weight, and radiated power of the system, but also mitigates electromagnetic interference and alleviates spectral scarcity [13]. As a result, researchers have begun considering not just the coexistence of radar and communications, but more fundamentally schemes of integrated radar and communication system [1]. In [14], the radar MI and communication channel capacity of a MIMO-based integrated radar and communication system are analyzed, where the effects of signal-to-noise ratio (SNR) and the number of antennas on the system performance are revealed. In the integrated system, it is of great importance to design waveform to enhance resource utilization efficiency. The authors in [13] propose an adaptive OFDM integrated radar and communications waveform design approach to improve the MI and data information rate for the integrated system. In [12], Chalise *et al.* present a performance tradeoff analysis for a joint bistatic passive radar and communication system, whose purpose is to optimally allocate power resource for transmitting radar waveform and communication signal in such a way that the probability of detection is maximized. Subsequently, reference [15] extends the work in [12] to a multiple-transmitter case. Also, the problem of secrecy communication for an integrated MIMO radar and communication system is investigated [16], where the primary goals of the radar are to guarantee a specified target detection performance and to simultaneously communication in security with a legitimate receiver by maximizing the secrecy rate against the eavesdropper.

Generally speaking, the vast majority of existing works concentrate on techniques to optimize the performance of radar target detection/tracking and communication rate for the integrated radar and communication system, without paying much attention to the problem of low probability of intercept (LPI). In real application, LPI optimization is a crucial part of military operations in hostile environments [17]–[19], for instance, the airborne integrated system is required to maintain LPI performance. In these scenarios, minimizing the radiated power that is required to perform the predefined task is essential and important [20]. The problem of resource allocation for multiple target tracking in MIMO radar systems is addressed in [21]–[25], wherein it is shown that the resource utilization efficiency can be improved remarkably. A pioneer LPI optimization for a joint bistatic radar and communication system is introduced in [26], where the authors minimize the total transmitted power for desired requirements of radar target detection and communication rate. However, the study in [26] focuses only on the integrated bistatic system. For the multistatic case, the limitations and derivations are much more complicated. To the best of our knowledge, there is no previous work regarding LPI-based optimal power allocation (LPI-OPA) in an integrated

multistatic radar and communication system until now. The need for LPI performance optimization in the underlying system is further emphasized, because more radiated energy might result in electronic or physical attacks in modern battlefield. Hence, in this paper, we will extend the results in [12], [15], and [26] and propose an LPI-OPA strategy for an integrated multistatic radar and communication system. These aspects render this model particularly attractive for offence applications, where the loader of the system needs to achieve LPI performance.

B. Main Contributions

For clarity, the major contributions of this paper are summarized as follows.

1) We formulate the system model for an integrated multistatic radar and communication system and derive the generalized likelihood ratio test (GLRT) detector, which is an extension of the work in [12], [15], and [26]. The integrated system is composed of multiple transmitters operating at different frequencies, a radar receiver (RR), and a communication receiver (CR). It is capable of fulfilling the requirements of both target detection and information transferring. Each transmitter utilizes a portion of its power resource to radiate a radar waveform, and another portion to broadcast a communication signal. The dedicated transmitters are able to detect the threat targets as well as transfer information to a CR. It is much different from the dual function system [27], which transmits the same signal for both functions at the transmitter. In this paper, the transmit power budget of each transmitter in the integrated system is allocated for transmitting radar waveform and information signal with the aim of enhancing its LPI performance, while satisfying the desired requirements of target detection and information rate.

2) The problem of LPI-OPA for an integrated multistatic radar and communication system is investigated. As previously mentioned, the work in [12] concentrates on the problem of performance tradeoff analysis for an integrated bistatic radar and communication system, and reference [15] extends it to a multistatic case. Specifically, in [15], the total transmit power at each transmitter is allocated for transmitting the radar waveforms and information signals in such a way that the probability of detection is maximized, while satisfying a predefined information rate requirement of the CR. To this end, only the transmit power allocated for the information signals is minimized, while all the remaining power resource is exploited to improve the target detection performance. Thus, the aim of both studies in [12] and [15] is to improve the target detection performance via power allocation (PA), whereas the LPI performance of the underlying system is ignored. On the other hand, in [26], the LPI-based PA scheme is only developed for a bistatic integrated system, which is much different from the multistatic scenario. Mathematically speaking, the LPI-OPA scheme is built in this paper to improve the LPI performance of the underlying system. Thus, it is actually an optimization problem of minimizing an objective function about the total power consumption of the integrated system while guaranteeing a predetermined target detection performance for the RR and a specified information rate for the CR. Since the analytical closed-form expression of the probability of detection is not tractable, its upper bound is derived.

3) We analytically show that the resulting LPI-OPA optimization scheme can be reformulated as two sub-problems, which can be solved by an efficient solution procedure based on the method of linear programming and the Karush–Kuhn–Tuckers (KKT) optimality conditions [28], [29].

4) Numerical results demonstrate the superiority of the presented LPI-OPA scheme compared to other existing PA algorithms. It is illustrated that the LPI-OPA scheme tends to allocate more power resource to the transmitter with better channel condition. In addition, it is also shown that the LPI performance of the integrated system can be remarkably enhanced by exploiting the LPI-OPA scheme.

C. Organization

The rest of this paper is structured as follows. Section II formulates the considered integrated multistatic radar and communication system model as well as the underlying assumptions needed in this paper. The LPI-OPA scheme is developed for an integrated multistatic radar and communication system in Section III. In Section III-A, the basis of the LPI-OPA optimization scheme is introduced. Section III-B derives the GLRT detector and the bound of probability of target detection. Then, the mathematical optimization framework of the LPI-OPA scheme is built in Section III-C, and the resulting constrained problem is equivalently converted as two subproblems, and then solved by the method of linear programming and the KKT conditions. Several numerical simulations are provided in Section IV to evaluate the accuracy of the theoretical derivations and substantiate the effectiveness of the proposed LPI-OPA scheme. Finally, the concluding remarks of the paper are made in Section V.

Notations: Unless otherwise specified, column vectors are represented by bold lower case letters (i.e., $\mathbf{x}$), matrices are denoted by bold upper case letters (i.e., $\mathbf{X}$), and scalars are denoted by normal font (i.e., x). The superscripts $(\cdot)^T$ and $(\cdot)^H$ indicate the transpose and Hermitian transpose, respectively. The superscript $(\cdot)^*$ indicates the optimality. $\mathbf{I}$ denotes the identity matrix, and $\| \cdot \|$ represents the Euclidean norm for vector or Frobenius norm for matrix. $\mathcal{CN}(\mu, \sigma^2)$ stands for Gaussian distribution with mean μ and variance σ^2. $\xi_{\max}(\mathbf{X})$ denotes the maximum eigenvalue of matrix $\mathbf{X}$, and $\mathbb{E}\{\cdot\}$ denotes the expectation operation. $\mathbb{P}\{\cdot\}$ is the probability operator.

II. SYSTEM MODEL

In this paper, we consider an integrated multistatic radar and communication system with M_T transmitters operating at different frequencies, an RR, and a CR, as depicted in Fig. 1. These dedicated transmitters are labeled $1, 2, \ldots, M_T (M_T \geq 2)$. Since the clutter signals have no Doppler shifts, they are located around the zero Doppler zone in the matched filtering [30]. Thus, the clutter signals can be mitigated by utilizing a large number of adaptive filters, such as the least-squares filter, normalized least mean squares filter, and so on. We consider a clutter-free noise-only environment, which can provide an upper bound for the detectors.

The underlying system is capable of fulfilling the requirements of both target detection and information transferring. In the scenario under consideration, the dedicated transmitters simultaneously radiate radar probing waveforms to the threat targets and communication signals to the CR [12], [15]. The ith transmitter utilizes a portion of its power resource, $P_{\mathrm{rad},i}$, to
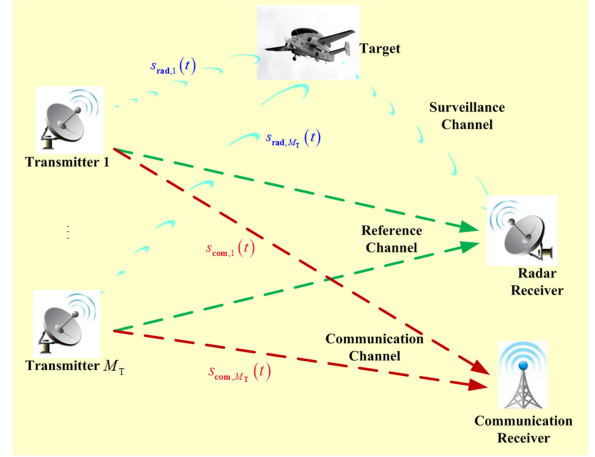

Fig. 1. Integrated multistatic radar and communication system with multiple transmitters, an RR, and a CR.

radiate a radar waveform $s_{\mathrm{rad},i}(t)$, and another portion, $P_{\mathrm{com},i}$, to broadcast a communication signal $s_{\mathrm{com},i}(t)$. For simplicity, it is also assumed that the signal transmissions from each transmitter are optimally scheduled by utilizing nonoverlapping groups of resource element (frequency) units. Physically speaking, some element units are employed to transmit radar waveform, while the other element units are used to broadcast information signal. On the other hand, by exploiting nonoverlapping frequency units, the different transmitters are able to radiate radar signals and communication signals at the same time, such that the interference received by the RR and CR is minimized.

At the RR, adaptive beamforming technique is utilized to separate the observed signals from each transmitter into surveillance channel (transmitter-target-RR) and reference channel (transmitter-RR) signals. It is also supposed that the dedicated transmitters and RR antennas are directional. In such a case, the target position is known as *a priori* knowledge, which can be determined by utilizing the multiframe detection approaches or maximum likelihood-probabilistic data association technique. The reference channel signal can be exploited to estimate the radar waveform at the RR, where the time difference of arrival between the two channels can be computed through a correlation between the surveillance channel and reference channel signals [26]. In real scenario, the high SNR of the reference channel, which are common in practice [31], can be achieved by pointing directional transmitting beams at the RR. In this way, the presence of the high SNR of the reference channel cannot degrade the LPI performance of the integrated system.

Herein, the information rate in nats per channel use (npcu) is defined and subsequently utilized as a metric for communication requirement at the CR, which can be expressed by

$$R_{\mathrm{com}} = \frac{1}{M_T} \sum_{i=1}^{M_T} \log(1 + P_{\mathrm{com},i}\gamma_{\mathrm{com},i}) \qquad (1)$$

where $P_{\mathrm{com},i}$ denotes the transmit power allocated for the information waveforms at the ith transmitter, $\gamma_{\mathrm{com},i}$ represents the channel coefficient at the CR corresponding to the ith transmitter, and $P_{\mathrm{com},i}\gamma_{\mathrm{com},i}$ represents the instantaneous SNR at the CR. Mathematically, $\gamma_{\mathrm{com},i}$ is the ratio of the squared absolute value of the ith transmitter-CR channel to the variance of the additive noise at the CR, which incorporates the transmitting and

receiving antenna gains, the attenuation in the channel and the noise power [12]. It is also supposed that, for convenience, the communication signals scattered off the target are not utilized for target detection at the CR, which are much weaker than the communication channels from the transmitters and can be ignored.

Remark 1: In the current paper, we focus on the problem of LPI-based PA for an integrated multistatic radar and communication system, where the total radiated power is minimized by optimizing the transmit PA at each transmitter for radar waveforms and information signals. Since the dedicated transmitters operate at different frequencies, the RF spectrum should also be optimized to detect targets and transfer information, which is beyond the scope of this paper. The joint optimization of transmit power and RF spectrum allocation will be studied in the near future.

III. LPI Performance Optimization Scheme

A. Basis of the Technique

Mathematically speaking, the LPI-OPA scheme for an integrated multistatic radar and communication system can be formulated as a problem of optimizing the transmit PA to minimize the total power consumption of the integrated system for both radar waveforms and information signals, respectively, subject to a predetermined target detection performance for the RR and a desired information rate for the CR. First, the GLRT detector is derived, where the upper bound of the probability of detection is calculated due to the fact that its analytical expression is not tractable. Then, we analytically show that the resulting optimization problem can equivalently be converted to two subproblems, which can be solved by an efficient solution procedure based on the method of linear programming and the KKT conditions.

We are now in a position to design and control the transmit power of different transmitters in order to achieve better LPI performance for an integrated multistatic radar and communication system. The general LPI-OPA optimization can be detailed as follows.

B. GLRT Detector

Without loss of generality, we consider a single target scenario. Given the discussions in previous sections, the target detection problem in the integrated multistatic radar and communication system can be formulated as the following binary hypothesis test between target presence $\mathcal{H}_1$ and null $\mathcal{H}_0$ hypotheses [12], [15]:

$$\mathcal{H}_0 : \begin{cases} \mathbf{y}_{\mathrm{ref},i} = \gamma_{\mathrm{ref},i}\mathbf{W}_{\mathrm{ref},i}\mathbf{s}_{\mathrm{rad},i} + \mathbf{v}_{\mathrm{ref},i} \\ \mathbf{y}_{\mathrm{sur},i} = \mathbf{v}_{\mathrm{sur},i} \end{cases} \quad (2)$$

$$\mathcal{H}_1 : \begin{cases} \mathbf{y}_{\mathrm{ref},i} = \gamma_{\mathrm{ref},i}\mathbf{W}_{\mathrm{ref},i}\mathbf{s}_{\mathrm{rad},i} + \mathbf{v}_{\mathrm{ref},i} \\ \mathbf{y}_{\mathrm{sur},i} = \gamma_{\mathrm{sur},i}\mathbf{W}_{\mathrm{sur},i}\mathbf{s}_{\mathrm{rad},i} + \mathbf{v}_{\mathrm{sur},i} \end{cases} \quad (3)$$

where $\mathbf{y}_{\mathrm{ref},i}$ and $\mathbf{y}_{\mathrm{sur},i}$ are the radar signals observed from the ith transmitter corresponding to the reference and surveillance channels, respectively; $\gamma_{\mathrm{ref},i}$ and $\gamma_{\mathrm{sur},i}$ are the channel coefficients corresponding to the ith reference and surveillance channels, respectively; $\mathbf{W}_{\mathrm{ref},i}$ and $\mathbf{W}_{\mathrm{sur},i}$ represent the $K \times K$ unitary delay-Doppler operator matrices corresponding to the

ith reference and surveillance channels, respectively, and K is the length of the received signals; $\mathbf{s}_{\mathrm{rad},i}$ denotes the $K \times 1$ vector of sampled radar signal $s_{\mathrm{rad},i}(t)$, and the transmit power is $\|s_{\mathrm{rad},i}(t)\|^2 = P_{\mathrm{rad},i}$; Finally, $\mathbf{v}_{\mathrm{ref},i}$ and $\mathbf{v}_{\mathrm{sur},i}$ denote the RR noise at the antennas used for reference and surveillance channels, respectively.

Generally, the parameters $\mathbf{s}_{\mathrm{rad},i}$, $\gamma_{\mathrm{ref},i}$ and $\gamma_{\mathrm{sur},i}$ are not known. For known positions of the transmitters, and position and velocity of the target at a range-Doppler cell (hypothesized position), the delay-Doppler operator matrices $\mathbf{W}_{\mathrm{ref},i}$ and $\mathbf{W}_{\mathrm{sur},i}$ can be calculated. In addition, owing to the property of unitary matrix, we have $\mathbf{W}_{\mathrm{ref},i}\mathbf{W}_{\mathrm{ref},i}^H = \mathbf{W}_{\mathrm{sur},i}\mathbf{W}_{\mathrm{sur},i}^H = \mathbf{I}$, $\forall i$. Then, after unitary transformations with $\mathbf{W}_{\mathrm{ref},i}$ and $\mathbf{W}_{\mathrm{sur},i}$, (2) and (3) can equivalently be reformulated in the following:

$$\mathcal{H}_0 : \begin{cases} \widetilde{\mathbf{y}}_{\mathrm{ref},i} = \gamma_{\mathrm{ref},i}\mathbf{s}_{\mathrm{rad},i} + \widetilde{\mathbf{v}}_{\mathrm{ref},i} \\ \widetilde{\mathbf{y}}_{\mathrm{sur},i} = \widetilde{\mathbf{v}}_{\mathrm{sur},i} \end{cases} \quad (4)$$

$$\mathcal{H}_1 : \begin{cases} \widetilde{\mathbf{y}}_{\mathrm{ref},i} = \gamma_{\mathrm{ref},i}\mathbf{s}_{\mathrm{rad},i} + \widetilde{\mathbf{v}}_{\mathrm{ref},i} \\ \widetilde{\mathbf{y}}_{\mathrm{sur},i} = \gamma_{\mathrm{sur},i}\mathbf{s}_{\mathrm{rad},i} + \widetilde{\mathbf{v}}_{\mathrm{sur},i} \end{cases} \quad (5)$$

where $\widetilde{\mathbf{y}}_{\mathrm{ref},i} \triangleq \mathbf{W}_{\mathrm{ref},i}^H\mathbf{y}_{\mathrm{ref},i}$, $\widetilde{\mathbf{y}}_{\mathrm{sur},i} \triangleq \mathbf{W}_{\mathrm{sur},i}^H\mathbf{y}_{\mathrm{sur},i}$. $\widetilde{\mathbf{v}}_{\mathrm{ref},i} = \mathbf{W}_{\mathrm{ref},i}^H\mathbf{v}_{\mathrm{ref},i}$ and $\widetilde{\mathbf{v}}_{\mathrm{sur},i} = \mathbf{W}_{\mathrm{sur},i}^H\mathbf{v}_{\mathrm{sur},i}$ represent the additive zero-mean white Gaussian noise with variance matrix $\sigma^2\mathbf{I}$, i.e., $\widetilde{\mathbf{v}}_{\mathrm{ref},i} \sim \mathcal{CN}(\mathbf{0}, \sigma^2\mathbf{I})$, $\widetilde{\mathbf{v}}_{\mathrm{sur},i} \sim \mathcal{CN}(\mathbf{0}, \sigma^2\mathbf{I})$.

In order to design an efficient detector for the hypothesis testing, the GLRT detector is employed here by exploiting the signal model described in the previous section, which is similar to the Neyman–Pearson detector as the number of samples approaches infinity [33]. Based on the above definitions, the joint probability density functions (PDFs) of $\widetilde{\mathbf{y}}_{\mathrm{ref}}$ and $\widetilde{\mathbf{y}}_{\mathrm{sur}}$ under the hypotheses $\mathcal{H}_0$ and $\mathcal{H}_1$ respectively, can be expressed as

$$f((\widetilde{\mathbf{y}}_{\mathrm{ref}}, \widetilde{\mathbf{y}}_{\mathrm{sur}})|\mathcal{H}_0)$$
$$= \frac{1}{(\pi\sigma^2)^{(M_{\mathrm{T}}+1)K}}\exp\left[\frac{-\sum_{i=1}^{M_{\mathrm{T}}}\left(\|\overline{\mathbf{y}}_{\mathrm{ref},i}\|^2 + \|\widetilde{\mathbf{y}}_{\mathrm{sur},i}\|^2\right)}{\sigma^2}\right] \quad (6)$$

and

$$f((\widetilde{\mathbf{y}}_{\mathrm{ref}}, \widetilde{\mathbf{y}}_{\mathrm{sur}})|\mathcal{H}_1)$$
$$= \frac{1}{(\pi\sigma^2)^{(M_{\mathrm{T}}+1)K}}\exp\left[\frac{-\sum_{i=1}^{M_{\mathrm{T}}}\left(\|\overline{\mathbf{y}}_{\mathrm{ref},i}\|^2 + \|\overline{\mathbf{y}}_{\mathrm{sur},i}\|^2\right)}{\sigma^2}\right] \quad (7)$$

where $\widetilde{\mathbf{y}}_{\mathrm{ref}} = [\mathbf{y}_{\mathrm{ref},1}^T, \ldots, \mathbf{y}_{\mathrm{ref},M_{\mathrm{T}}}^T]^T$, $\widetilde{\mathbf{y}}_{\mathrm{sur}} = [\mathbf{y}_{\mathrm{sur},1}^T, \ldots, \mathbf{y}_{\mathrm{sur},M_{\mathrm{T}}}^T]^T$, $\overline{\mathbf{y}}_{\mathrm{ref},i} = \widetilde{\mathbf{y}}_{\mathrm{ref},i} - \gamma_{\mathrm{ref},i}\mathbf{s}_{\mathrm{rad},i}$, and $\overline{\mathbf{y}}_{\mathrm{sur},i} = \widetilde{\mathbf{y}}_{\mathrm{sur},i} - \gamma_{\mathrm{sur},i}\mathbf{s}_{\mathrm{rad},i}$

Subsequently, the target detection problem can be formulated and solved by comparing the likelihood ratio test function as follows:

$$\Gamma(\widetilde{\mathbf{y}}_{\mathrm{ref}}, \widetilde{\mathbf{y}}_{\mathrm{sur}}) = \frac{f((\widetilde{\mathbf{y}}_{\mathrm{ref}}, \widetilde{\mathbf{y}}_{\mathrm{sur}})|\mathcal{H}_1)}{f((\widetilde{\mathbf{y}}_{\mathrm{ref}}, \widetilde{\mathbf{y}}_{\mathrm{sur}})|\mathcal{H}_0)} \underset{\mathcal{H}_0}{\overset{\mathcal{H}_1}{\gtrless}} \delta \quad (8)$$

where $\delta \in [0, 1]$ denotes a certain threshold value, which can be determined by a specified probability of false alarm p_{FA}. As previously stated, since the parameters $\mathbf{s}_{\mathrm{rad},i}$, $\gamma_{\mathrm{ref},i}$, and $\gamma_{\mathrm{sur},i}$ are unknown, they can be substituted with their maximum-likelihood (ML) estimates in the likelihood ratio test function

(8) to obtain a new test function, i.e., GLRT function [15]. According to the derivations in [15], the GLRT function becomes

$$\log \Gamma(\widetilde{\mathbf{y}}_{\mathrm{ref}}, \widetilde{\mathbf{y}}_{\mathrm{sur}}) = \frac{1}{\sigma^2} \sum_{i=1}^{M_{\mathrm{T}}} \left[\xi_{\max}(\mathbf{Z}_i) - \|\widetilde{\mathbf{y}}_{\mathrm{ref},i}\|^2 \right] \quad (9)$$

where $\mathbf{Z}_i \triangleq \widetilde{\mathbf{y}}_{\mathrm{ref},i} \widetilde{\mathbf{y}}_{\mathrm{ref},i}^H + \widetilde{\mathbf{y}}_{\mathrm{sur},i} \widetilde{\mathbf{y}}_{\mathrm{sur},i}^H$, and $\xi_{\max}(\mathbf{Z}_i)$ denotes the maximum eigenvalue of matrix $\mathbf{Z}_i$. Hence, the ML estimates of parameters $\gamma_{\mathrm{ref},i}$ and $\gamma_{\mathrm{sur},i}$ can be obtained from

$$\max_{\gamma_{\mathrm{ref},i}, \gamma_{\mathrm{ref},i}, \forall i} \log \Gamma(\widetilde{\mathbf{y}}_{\mathrm{ref}}, \widetilde{\mathbf{y}}_{\mathrm{sur}}). \quad (10)$$

In order to analyze the target detection performance of the underlying integrated system, the probabilities of detection and false alarm should be derived. With (11), the probability of detection p_{D} can be given by

$$p_{\mathrm{D}} = \mathbb{P} \left\{ \frac{1}{\sigma^2} \sum_{i=1}^{M_{\mathrm{T}}} \left[\xi_{\max}(\mathbf{Z}_i) - \|\widetilde{\mathbf{y}}_{\mathrm{ref},i}\|^2 \right] \geq \delta | \mathcal{H}_1 \right\} \quad (11)$$

where $(\cdot)|\mathcal{H}_1$ represents that $(\cdot)$ is conditioned on $\mathcal{H}_1$, and $\mathbf{Z}_i \triangleq \widetilde{\mathbf{y}}_{\mathrm{ref},i} \widetilde{\mathbf{y}}_{\mathrm{ref},i}^H + \widetilde{\mathbf{y}}_{\mathrm{sur},i} \widetilde{\mathbf{y}}_{\mathrm{sur},i}^H$. Based on the discussions in [15], there do not exist the analytical closed-form expression for p_{D}, even though the statistical distributions of $\xi_{\max}(\mathbf{Z}_i)$ and $\|\widetilde{\mathbf{y}}_{\mathrm{ref},i}\|^2$ are exactly known. In such a scenario, we can get the upper bound of probability of detection by applying the Markov's inequality [15]

$$p_{\mathrm{D}} \leq \mathbb{E} \left\{ \frac{1}{\delta\sigma^2} \sum_{i=1}^{M_{\mathrm{T}}} \left[\xi_{\max}(\mathbf{Z}_i) - \|\widetilde{\mathbf{y}}_{\mathrm{ref},i}\|^2 \right] | \mathcal{H}_1 \right\}. \quad (12)$$

After algebraic manipulations, the upper bound of p_{D} boils down to

$$p_{\mathrm{D}} \leq \frac{1}{\delta\sigma^2} \sum_{i=1}^{M_{\mathrm{T}}} \left\{ |\gamma_{\mathrm{sur},i}|^2 P_{\mathrm{rad},i} - (K-2)\sigma^2 \right\} \triangleq \overline{p_{\mathrm{D}}} \quad (13)$$

where the detailed derivations can be found in [15].

Furthermore, it is assumed that the SNR of the reference channel is high. As mentioned before, it is common and can be achieved in practice. Then, the probability of false alarm p_{FA} can be expressed by [32]

$$p_{\mathrm{FA}} \simeq \int_{2\delta}^{\infty} \frac{1}{2^{M_{\mathrm{T}}} \Gamma(M_{\mathrm{T}})} x^{M_{\mathrm{T}}-1} e^{-\frac{x}{2}} dx = \frac{\Gamma(M_{\mathrm{T}}, \delta)}{\Gamma(M_{\mathrm{T}})} \quad (14)$$

where $\Gamma(M_{\mathrm{T}}) = \int_0^{\infty} t^{M_{\mathrm{T}}-1} e^{-t} dt$ denotes Gamma function, and $\Gamma(M_{\mathrm{T}}, \delta) = \int_{\delta}^{\infty} t^{M_{\mathrm{T}}-1} e^{-t} dt$ denotes the upper incomplete Gamma function. From (14), it can be seen that, for a specified probability of false alarm, the threshold value δ can numerically be calculated.

Remark 2: According to (13) and (14), one can notice that, the target detection performance can be evaluated by adopting the probabilities of detection and false alarm. Mathematically speaking, for a fixed p_{FA}, increasing the radiated power of each transmitter can enlarge the value of $\overline{p_{\mathrm{D}}}$, implying better target detection performance. However, it will in turn increase the vulnerability of the integrated multistatic radar and communication system in modern battlefield. Therefore, we develop an LPI-OPA scheme by optimizing the PA to minimize the total radiated power consumption, while meeting specified requirements of target detection and communication rate, as presented in the next subsection.

C. LPI-OPA Model

For a predefined target detection performance for the RR and a desired information rate for the CR, the intention of this paper is to optimally allocate the power resource which can result in the minimization of the total radiated power. In such a model, the LPI performance of the integrated system can markedly be enhanced. The resulting optimization problem can be formulated mathematically as follows:

$$(\mathbf{P}): \min_{P_{\mathrm{rad},i}, P_{\mathrm{com},i}, \forall i} \sum_{i=1}^{M_{\mathrm{T}}} (P_{\mathrm{rad},i} + P_{\mathrm{com},i}) \quad (15a)$$

$$\text{s.t.}: \begin{cases} \mathbf{C1}: p_{\mathrm{FA}} \leq \delta_{\mathrm{FA}} \\ \mathbf{C2}: \overline{p_{\mathrm{D}}} \geq \delta_{\mathrm{D}} \\ \mathbf{C3}: R_{\mathrm{com}} \geq r_{\mathrm{com}} \\ \mathbf{C4}: P_{\mathrm{rad},i} + P_{\mathrm{com},i} \leq P_{\mathrm{tot},i}, \forall i \\ \mathbf{C5}: P_{\mathrm{rad},i} \geq 0, P_{\mathrm{com},i} \geq 0, \forall i. \end{cases} \quad (15b)$$

The first constraint $\mathbf{C1}$ stands that the probability of false alarm p_{FA} is less than a predetermined threshold value δ_{FA}, while the second constraint $\mathbf{C2}$ stands that the upper bound of the probability of detection $\overline{p_{\mathrm{D}}}$ should be greater than a given threshold value δ_{D}, such that the desired target detection performance for the RR is satisfied. The third constraint $\mathbf{C3}$ represents that the information rate for the CR is above the threshold r_{com} to meet the communication requirement. The last two constraints $\mathbf{C4}$ and $\mathbf{C5}$ imply that the transmit power of each transmitter is constrained by a minimum and maximum value, where $P_{\mathrm{tot},i}$ denotes the maximum transmit power of the ith transmitter.

Note that the primary objective of this paper is to guarantee a predefined target detection performance for the RR and a given information rate for the CR respectively, while minimizing the total radiated power through optimal PA at each transmitter for radar waveforms and information signals. Hence, the available maximum transmit power of each transmitter $P_{\mathrm{tot},i}$ ($\forall i$) should be large enough to perform both radar and communication functions. Otherwise, neither the target detection requirement of the RR nor the information rate requirement of the CR could be satisfied. In such a case, the adaptable parameters $P_{\mathrm{rad},i}$ and $P_{\mathrm{com},i}$ are not coupled. Then, the optimization problem $\mathbf{P}$ can equivalently be recast as the following two subproblems:

$$(\mathbf{SP1}): \min_{P_{\mathrm{rad},i}, \forall i} \sum_{i=1}^{M_{\mathrm{T}}} P_{\mathrm{rad},i} \quad (16a)$$

$$\text{s.t.}: \begin{cases} \mathbf{C1}: p_{\mathrm{FA}} \leq \delta_{\mathrm{FA}} \\ \mathbf{C2}: \overline{p_{\mathrm{D}}} \geq \delta_{\mathrm{D}} \\ \mathbf{C4}: P_{\mathrm{rad},i} \leq P_{\mathrm{tot},i} - P_{\mathrm{com},i}, \forall i \\ \mathbf{C5}: P_{\mathrm{rad},i} \geq 0, \forall i \end{cases} \quad (16b)$$

and

$$(\textbf{SP2}): \min_{P_{\text{com},i}, \forall i} \sum_{i=1}^{M_{\text{T}}} P_{\text{com},i} \tag{17a}$$

$$\text{s.t.} : \begin{cases} \textbf{C3} : R_{\text{com}} \geq r_{\text{com}} \\ \textbf{C4} : P_{\text{com},i} \leq P_{\text{tot},i} - P_{\text{rad},i}, \forall i \\ \textbf{C5} : P_{\text{com},i} \geq 0, \forall i. \end{cases} \tag{17b}$$

From the subproblem (**SP1**), it is obvious that the optimal transmit power for radar waveform $P_{\text{rad},i}$ can be obtained when "=" in the constraint **C1** holds. Subsequently, the underlying subproblem described in (16) is a typical linear programming problem [34], [35]. Thus, the exact solution $P_{\text{rad},i}^*$ can be solved by several convex optimization algorithms, such as the interior point approach. After that, this optimal solution $P_{\text{rad},i}^*$ is applied to solve the remaining subproblem (**SP2**).

To further proceed to solve the optimization problem (**SP2**), the following necessary proposition should first be noted.

Proposition 3.1: The optimization problem (**SP2**) is convex, with the following properties: (a) R_{com} is a monotonic increasing function of $P_{\text{com},i}$; (b) The first derivative of $\frac{\partial R_{\text{com}}}{\partial P_{\text{com},i}}$ is monotonic decreasing in $P_{\text{com},i}$.

Proof: Taking the derivative of R_{com} with respect to $P_{\text{com},i}$, we can obtain

$$\frac{\partial R_{\text{com}}}{\partial P_{\text{com},i}} = \frac{1}{M_{\text{T}}} \cdot \frac{\gamma_{\text{com},i}}{1 + P_{\text{com},i}\gamma_{\text{com},i}} > 0, \forall i. \tag{18}$$

Then we have

$$\frac{\partial^2 R_{\text{com}}}{\partial P_{\text{com},i}^2} = -\frac{1}{M_{\text{T}}} \cdot \frac{\gamma_{\text{com},i}^2}{(1 + P_{\text{com},i}\gamma_{\text{com},i})^2} < 0. \tag{19}$$

From the above derivations, we can see that (18) implies the increasing nature of R_{com} with respect to $P_{\text{com},i}$, and (19) indicates the decreasing nature of the first derivative of $\frac{\partial R_{\text{com}}}{\partial P_{\text{com},i}}$ with respect to $P_{\text{com},i}$. Additionally, (18) and (19) show that the Hessian matrix of the information rate (1) with respect to $P_{\text{com},i}$ is a diagonal matrix with nonpositive elements. Hence, it is shown that the information rate R_{com} is increasing and concave with respect to $P_{\text{com},i}$.

As a consequence, the constraint **C3** constitutes a convex feasible set over $P_{\text{com},i}$, while the objective function is affine and the power constraints **C4** and **C5** are the intersection of $2M_{\text{T}}$ half-spaces, and hence convex [36], [37], which completes the proof. ∎

Traditionally, numerical optimization approaches, such as subgradient and gradient projection methods, can be employed to solve the aforementioned convex optimization problem (**SP2**). However, these traditional algorithms require iterative calculations and can only numerically achieve the optimal solution, that is, no closed-form expression can be obtained [38]. Thus, to derive the closed-form solution, we employ the method of Lagrange multipliers to solve the constrained convex optimization problem (17). Introducing Lagrange multipliers $\varphi_1 \geq 0$, $\varphi_2 \geq 0$, and $\varphi_3 \geq 0$ for the multiple constraints, the Lagrange of subproblem (**SP2**) can equivalently be written as

$$\mathcal{L}(P_{\text{com},i}, \varphi_1, \varphi_2, \varphi_3)$$

$$= \sum_{i=1}^{M_{\text{T}}} P_{\text{com},i} + \varphi_1 \cdot (-P_{\text{com},i}) + \varphi_2 \cdot [P_{\text{com},i} - (P_{\text{tot},i} - P_{\text{rad},i}^*)]$$

$$+ \varphi_3 \cdot \left[r_{\text{com}} - \frac{1}{M_{\text{T}}} \sum_{i=1}^{M_{\text{T}}} \log(1 + P_{\text{com},i}\gamma_{\text{com},i}) \right]. \tag{20}$$

It is worth noting that due to the convex nature of (**SP2**) the Karush–Kuhn–Tucker (KKT) conditions are the necessary and sufficient conditions for the global optimality $P_{\text{com},i}^*$ [29], and the Lagrange multipliers φ_1^*, φ_2^*, and φ_3^*. In order to solve the convex optimization problem (**SP2**), the KKT optimality conditions can be subsequently derived as follows for any optimal point $(P_{\text{com},i}^*, \varphi_1^*, \varphi_2^*, \varphi_3^*)$

$$\frac{\partial \mathcal{L}}{\partial P_{\text{com},i}^*} = 1 - \varphi_1^* + \varphi_2^* - \frac{\varphi_3^* \gamma_{\text{com},i}/M_{\text{T}}}{1 + P_{\text{com},i}^* \gamma_{\text{com},i}} = 0 \tag{21a}$$

$$\varphi_1^* \cdot (-P_{\text{com},i}^*) = 0 \tag{21b}$$

$$\varphi_2^* \cdot [P_{\text{com},i}^* - (P_{\text{tot},i} - P_{\text{rad},i}^*)] = 0 \tag{21c}$$

$$\varphi_3^* \cdot \left[r_{\text{com}} - \frac{1}{M_{\text{T}}} \sum_{i=1}^{M_{\text{T}}} \log(1 + P_{\text{com},i}^* \gamma_{\text{com},i}) \right] = 0 \tag{21d}$$

$$0 \leq P_{\text{com},i}^* \leq P_{\text{tot},i} - P_{\text{rad},i}^*, \forall i \tag{21e}$$

$$\varphi_1^* \geq 0 \tag{21f}$$

$$\varphi_2^* \geq 0 \tag{21g}$$

$$\varphi_3^* \geq 0. \tag{21h}$$

According to the KKT conditions, if $P_{\text{com},i}^*$ is the optimal solution, it must satisfy the stationarity condition $\frac{\partial \mathcal{L}}{\partial P_{\text{com},i}^*} = 0$, primal feasibility $\frac{1}{M_{\text{T}}} \sum_{i=1}^{M_{\text{T}}} \log(1 + P_{\text{com},i}^* \gamma_{\text{com},i}) \geq r_{\text{com}}$, $0 \leq P_{\text{com},i}^* \leq P_{\text{tot},i} - P_{\text{rad},i}^*$, dual feasibility $\varphi_1^* \geq 0, \varphi_2^* \geq 0, \varphi_3^* \geq 0$ and complementary slackness which states that a primal constraint is satisfied with equality, if and only if, the associated dual variable is strictly greater than zero [38].

From the stationary condition, when $P_{\text{com},i}^*$ is optimal, we obtain

$$P_{\text{com},i}^* = \frac{\varphi_3^*/M_{\text{T}}}{1 - \varphi_1^* + \varphi_2^*} - \frac{1}{\gamma_{\text{com},i}}. \tag{22}$$

It is apparent from (21a)–(21c) that the optimality conditions can be separately investigated for three possibilities regarding the optimal allocated power at each transmitter. At the optimality, each transmitter can be allocated either with no power (i.e., $P_{\text{com},i}^* = 0$), with maximum transmit power (i.e., $P_{\text{com},i}^* = P_{\text{tot},i} - P_{\text{rad},i}^*$), or with a power between these two extreme cases (i.e., $0 \leq P_{\text{com},i}^* \leq P_{\text{tot},i} - P_{\text{rad},i}^*$).

1) If $0 < P_{\text{com},i}^* < P_{\text{tot},i} - P_{\text{rad},i}^*$, then $\varphi_1^* = \varphi_2^* = 0$, we have

$$0 < \frac{\varphi_3^*}{M_{\text{T}}} - \frac{1}{\gamma_{\text{com},i}} < P_{\text{tot},i} - P_{\text{rad},i}^*$$

$$\Longleftrightarrow \frac{M_{\text{T}}}{\gamma_{\text{com},i}} < \varphi_3^* < M_{\text{T}} \left(P_{\text{tot},i} - P_{\text{rad},i} + \frac{1}{\gamma_{\text{com},i}} \right). \tag{23}$$

Then, $P^*_{\text{com},i}$ can be computed as

$$P^*_{\text{com},i} = \frac{\varphi^*_3}{M_T} - \frac{1}{\gamma_{\text{com},i}} \quad (24)$$

where φ^*_3 can be determined by

$$\frac{1}{M_T} \sum_{i=1}^{M_T} \log(1 + P^*_{\text{com},i}\gamma_{\text{com},i}) \geq r_{\text{com}}. \quad (25)$$

2) If $P^*_{\text{com},i} = 0$, then $\varphi^*_1 > 0$, $\varphi^*_2 = 0$, we can obtain

$$P^*_{\text{com},i} + \frac{1}{\gamma_{\text{com},i}} = \frac{\varphi^*_3/M_T}{1 - \varphi^*_1} > \varphi^*_3/M_T$$

$$\Longleftrightarrow \varphi^*_3 < \frac{M_T}{\gamma_{\text{com},i}}. \quad (26)$$

Then, $P^*_{\text{com},i}$ can be given by

$$P^*_{\text{com},i} = 0. \quad (27)$$

3) If $P^*_{\text{com},i} = P_{\text{tot},i} - P^*_{\text{rad},i}$, then $\varphi^*_1 = 0$, $\varphi^*_2 > 0$, we have

$$P^*_{\text{com},i} + \frac{1}{\gamma_{\text{com},i}} = \frac{\varphi^*_3/M_T}{1 + \varphi^*_2} < \varphi^*_3/M_T$$

$$\Longleftrightarrow \varphi^*_3 > M_T\left(P_{\text{tot},i} - P^*_{\text{rad},i} + \frac{1}{\gamma_{\text{com},i}}\right). \quad (28)$$

Then, $P^*_{\text{com},i}$ is obtained as

$$P^*_{\text{com},i} = P_{\text{tot},i} - P^*_{\text{rad},i}. \quad (29)$$

Therefore, the globally optimal PA solution for (**SP2**) can be obtained as (30), shown at the bottom of the this page, where φ^*_3 is a constant calculated by the predefined information rate of the CR

$$\frac{1}{M_T} \sum_{i=1}^{M_T} \log(1 + P^*_{\text{com},i}\gamma_{\text{com},i}) \geq r_{\text{com}}. \quad (31)$$

For the sake of clarity, the detailed steps of the LPI-OPA scheme are summarized in Algorithm 1 for the integrated multi-static radar and communication system, according to which we can obtain the optimal transmit PA for both radar waveform and communication signal. Moreover, it is worth to mention that φ^*_3 can be obtained by employing the well-known bisection search technique [10], which is shown in Algorithm 2.

Remark 3 (Complexity Analysis): As aforementioned, the subproblem (**SP1**) can be solved efficiently via the interior point approach with a computational complexity of $\mathcal{O}(M_T^{3.5})$. On the other hand, the iterative steps of bisection search technique to find φ^*_3 can be carried out by utilizing one-dimensional search over the parameter φ_3. The complexity of Algorithm 2 is dominated by the number of transmitters and the procedure

---

Algorithm 1: The Detailed Steps of the LPI-OPA Scheme.

Input: Set δ, δ_{FA}, δ_{D}, r_{com}, M_T, K, σ^2, $P_{\text{tot},i}$
Output: $P^*_{\text{rad},i}$, $P^*_{\text{com},i}$ $(\forall i)$

1 **for** $i = 1, \cdots, M_T$ **do**
2   Calculate $P^*_{\text{rad},i}$ through the approach of linear programming;
3   Calculate φ^*_3 by utilizing bisection search method;
4   Calculate $P^*_{\text{com},i}$ by solving (30);
5 **end**
6 Output the final solution;

Algorithm 2: Bisection Search of φ^*_3.

Input: Set $\varphi^{(n)}_3$, $\varphi_{3,\min}$, $\varphi_{3,\max}$, the tolerance $\varepsilon > 0$, the iterative index n
Output: φ^*_3

1 **while** $R^{(n)}_{com} - r_{com} < \varepsilon$ **do**
2   **for** $i = 1, \cdots, M_T$ **do**
3         $\varphi^*_3 \leftarrow (\varphi_{3,\min} + \varphi_{3,\max})/2$;
4   Calculate $P^{(n)}_{\text{com},i}$ from (30);
5   Update $R^{(n)}_{\text{com}} \leftarrow \frac{1}{M_T} \sum_{i=1}^{M_T} \log(1 + P^{(n)}_{\text{com},i}\gamma_{\text{com},i})$;
6   **if** $R^{(n)}_{com} > r_{com}$ **then**
7             $\varphi_{3,\max} \leftarrow \varphi^{(n)}_3$;
8             $\varphi^{(n)}_3 \leftarrow (\varphi_{3,\min} + \varphi_{3,\max})/2$;
9   **end**
10   **else**
11             $\varphi_{3,\min} \leftarrow \varphi^{(n)}_3$;
12             $\varphi^{(n)}_3 \leftarrow (\varphi_{3,\min} + \varphi_{3,\max})/2$;
13   **end**
14   Set $n \leftarrow n + 1$;
15   **end**
16 **end**
17 Output the final solution;

---

of bisection search approach, which is $\mathcal{O}(M_T\log_2[(\varphi_{3,\max} - \varphi_{3,\min})/\varepsilon])$. However, the exhaustive search has a computational complexity of $\mathcal{O}(M_T(\varphi^*_3 - \varphi_{3,\min})/\varepsilon)$. For instance, a system with $M_T = 6$, $\varphi_{3,\min} = 0$, $\varphi_{3,\max} = 10^4$, $\varphi^*_3 = 5 \times 10^2$, and $\varepsilon = 0.5$ requires only on the order of 85.7 iterations with the proposed method, whereas the exhaustive search approach will require on the order of 6000 iterations. This implies that our proposed algorithm requires only 1.43% of the iterations compared with the exhaustive search method. Moreover, it is noteworthy that remarkable computational saving can be obtained by employing the proposed scheme for large number of transmitters M_T and great threshold of information rate

$$P^*_{\text{com},i} = \begin{cases} 0, & \varphi^*_3 < \dfrac{M_T}{\gamma_{\text{com},i}}, \\[2mm] \dfrac{\varphi^*_3}{M_T} - \dfrac{1}{\gamma_{\text{com},i}}, & \dfrac{M_T}{\gamma_{\text{com},i}} < \varphi^*_3 < M_T\left(P_{\text{tot},i} - P^*_{\text{rad},i} + \dfrac{1}{\gamma_{\text{com},i}}\right) \\[2mm] P_{\text{tot},i} - P^*_{\text{rad},i}, & \varphi^*_3 > M_T\left(P_{\text{tot},i} - P^*_{\text{rad},i} + \dfrac{1}{\gamma_{\text{com},i}}\right) \end{cases} \quad (30)$$
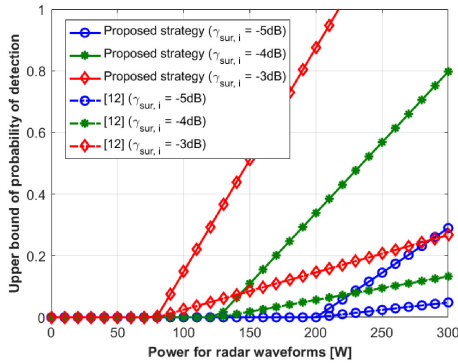
Fig. 2. Upper bound of probability of detection $\overline{p_{\rm D}}$ versus transmit power allocated for radar waveforms $P_{{\rm rad},i}$ with different $\gamma_{{\rm sur},i}$ and $\delta_{\rm FA}$ by utilizing different methods.

$r_{\rm com}$. Therefore, the problem (**P**) has the total complexity of $\mathcal{O}\left(M_{\rm T}^{3.5} + M_{\rm T}\log_2[(\varphi_{3,\max} - \varphi_{3,\min})/\varepsilon]\right)$.

IV. SIMULATION RESULTS AND PERFORMANCE ANALYSIS

A. Numerical Setup

In all the simulations, we assume an integrated multistatic radar and communication system consisting of $M_{\rm T} = 6$ transmitters, an RR, and a CR. Before proceeding to set other parameters, we should first determine the probability of false alarm, where we set $\delta_{\rm FA} = 4.12 \times 10^{-5}$. Then, the corresponding target detection threshold value δ can be obtained as 20.7233. The length of the received signal is $K = 4$, and the variance of the zero-mean additive Gaussian noise is $\sigma^2 = 10$. The maximum transmit power of each transmitter is $P_{{\rm tot},i} = 1000\,{\rm W}(\forall i)$.

B. Numerical Analysis

In Fig. 2, we depict the upper bound of probability of detection $\overline{p_{\rm D}}$ with respect to the transmit power allocated for radar waveforms $P_{{\rm rad},i}$ with different $\gamma_{{\rm sur},i}$ by utilizing different methods. It can be observed that the target detection performance is improved with the increase of transmit power for radar waveforms. Also, the boundaries of the regions widen as $\gamma_{{\rm sur},i}$ goes up [26]. That is to say, the upper bound of probability of detection is increased more drastically with the increase in $\gamma_{{\rm sur},i}$ and $\delta_{\rm FA}$. Moreover, the probability of detection is markedly increased by employing the proposed strategy when compared with the algorithm in [12].

Fig. 3 shows the probability of false alarm $p_{\rm FA}$ versus threshold value δ by utilizing different methods. As expected, the probability of false alarm is decreased as the threshold value δ increases.

Moreover, the information rate $R_{\rm com}$ versus the transmit power allocated for information signals $P_{{\rm com},i}$ with different $\gamma_{{\rm com},i}$ by utilizing different methods is illustrated in Fig. 4. One can notice that the information rate increases when the transmit power allocated for information signals goes up. Also, the information rate can be increased as $\gamma_{{\rm com},i}$ increases. In addition, the information rate can be significantly increased by employing the proposed strategy when compared with the results in [12].

Fig. 5 depicts the upper bound of probability of detection $\overline{p_{\rm D}}$ versus information rate $R_{\rm com}$ with $\gamma_{{\rm sur},i} = -5\,{\rm dB}$, $\gamma_{{\rm com},i} = -5\,{\rm dB}$, and $\delta_{\rm FA} = 4.12 \times 10^{-5}$ by utilizing different
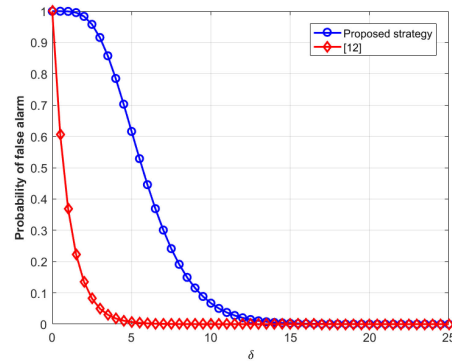

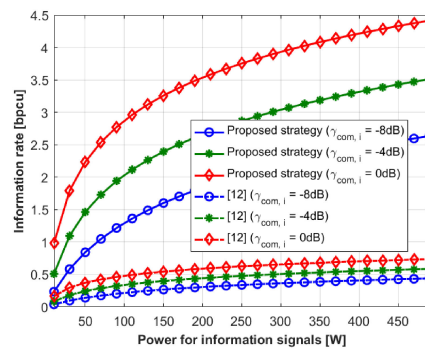Fig. 3. Probability of false alarm $p_{\rm FA}$ versus threshold value δ by utilizing different methods.

Fig. 4. Information rate $R_{\rm com}$ versus transmit power allocated for information signals $P_{{\rm com},i}$ with different $\gamma_{{\rm com},i}$ by utilizing different methods.
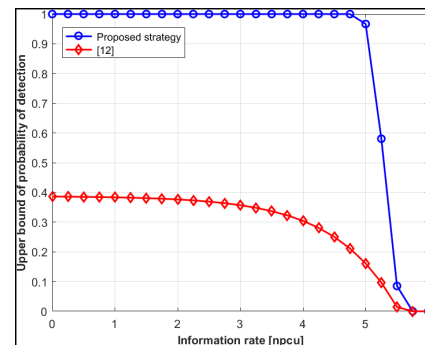

Fig. 5. Upper bound of probability of detection $\overline{p_{\rm D}}$ versus information rate $R_{\rm com}$ with $\gamma_{{\rm sur},i} = -5\,{\rm dB}$, $\gamma_{{\rm com},i} = -5\,{\rm dB}$, and $\delta_{\rm FA} = 4.12 \times 10^{-5}$ by utilizing different methods.

methods. This figure illustrates that the target detection performance degrades when the information rate is increased. It can also be found that the probability of detection is much larger with the same information rate threshold by using the proposed strategy than that in [12]. Thus, there exists a tradeoff between target detection performance and communications requirement.

C. PA Results

In this part, we aim to analyze the effects of several factors on the PA results. The coefficient values corresponding to surveillance channels are shown in Fig. 6. Fig. 7 depicts the
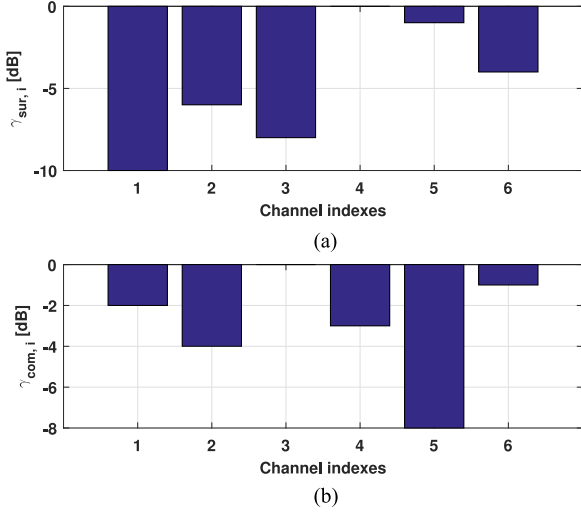
Fig. 6. Coefficient values for different channels. (a) Coefficients corresponding to the surveillance channels. (b) Coefficients corresponding to the communication channels.

transmit PA results achieved from our proposed scheme for different probabilities of detection and information rates. The results show that, to satisfy the requirements of both radar and communication subsystems, the integrated multistatic radar and communication system should properly distribute its transmit power to different transmitters: (a) More specifically, for a predetermined threshold of the probability of target detection, the LPI-OPA scheme only allocates its power resource to the transmitter with the best channel condition, that is, the largest channel coefficient value (see the PA results for Transmitter 4 for example). To guarantee a specified information rate for the CR, the proposed scheme tends to allocate more power resource to the transmitters with better channel conditions (see the PA results for Transmitter 1, Transmitter 3, and Transmitter 6 for example). Thus, the probability of target detection and information rate can be averaged. (b) Increasing the threshold values of the probability of detection p_{D} and information rate r_{com} can enlarge the total radiated power in the proposed LPI-OPA scheme, whereas the PA tendencies remain the same: the power resource tends to be assigned to the transmitters with better channel conditions (i.e., larger channel coefficient values). In this scenario, the power resource utilization efficiency can be enhanced [20].

D. Comparison of LPI Performance

To better examine the superiority of the proposed LPI-OPA scheme, the total radiated power of the proposed PA scheme is employed as a metric to compare with two existing PA models in Fig. 8 for different probabilities of detection and information rates, which is conducted through 10^5 Monte Carlo trials. Previously, authors have already presented two types of PA schemes—(1) maximize the probability of detection while meeting a desired information rate requirement of the CR, which is proposed by Chalise and denoted as CBK-OPA scheme [15]; (2) uniformly allocate the limited transmit power resource to multiple transmitters, which is denoted as the suboptimal PA scheme. In this scenario, the mathematical representation of the
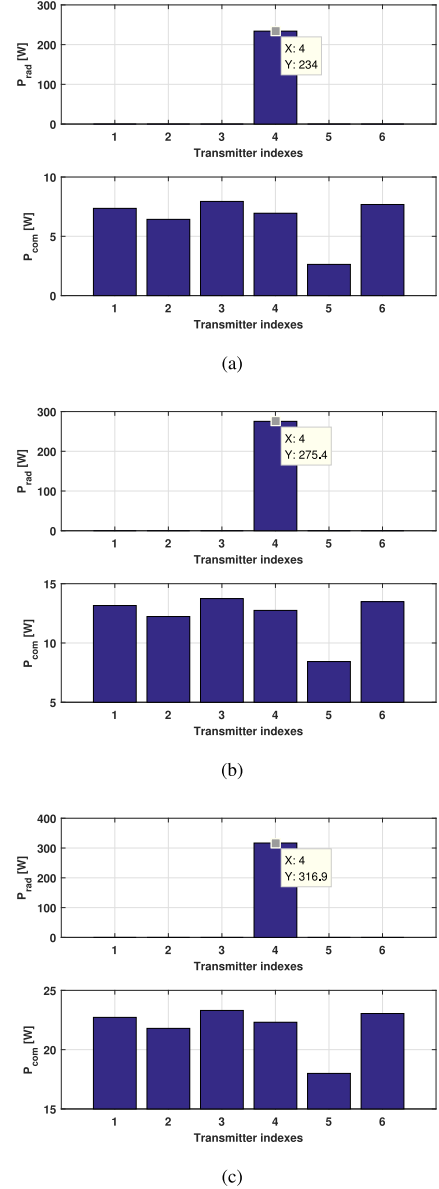

Fig. 7. LPI-OPA results for radar waveform and information rate: (a) $\delta_{\mathrm{D}} = 0.55, r_{\mathrm{com}} = 1.5$ npcu; (b) $\delta_{\mathrm{D}} = 0.75, r_{\mathrm{com}} = 2.0$ npcu; (c) $\delta_{\mathrm{D}} = 0.95$, $r_{\mathrm{com}} = 2.5$ npcu.

CBK-OPA model can be formulated as follows:

$$\text{CBK-OPA:} \quad \max_{P_{\mathrm{rad},i}, P_{\mathrm{com},i}, \forall i} \quad \overline{p_{\mathrm{D}}} \tag{32a}$$

$$\text{s.t. :} \quad \begin{cases} \mathbf{C1} : p_{\mathrm{FA}} \leq \delta_{\mathrm{FA}} \\ \mathbf{C3} : R_{\mathrm{com}} \geq r_{\mathrm{com}} \\ \mathbf{C4} : P_{\mathrm{rad},i} + P_{\mathrm{com},i} \leq P_{\mathrm{tot},i}, \forall i \\ \mathbf{C5} : P_{\mathrm{rad},i} \geq 0, P_{\mathrm{com},i} \geq 0, \forall i. \end{cases} \tag{32b}$$

Here, it is important to note that for a predetermined information rate requirement of the CR, the CBK-OPA algorithm minimizes the transmitted power for information signals, whereas all the remaining power resource is assigned to maximize the probability of detection. In this paper, the proposed LPI-OPA strategy
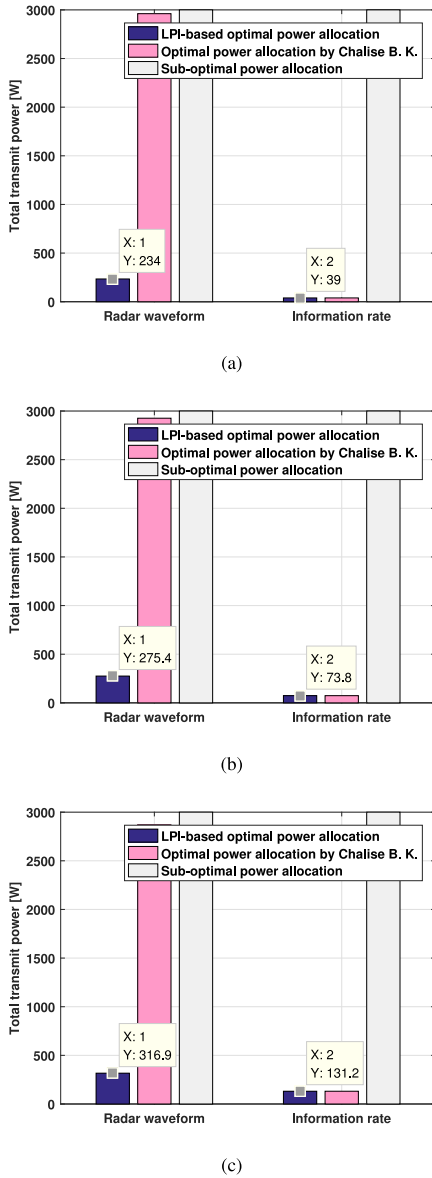
Fig. 8. Comparison of total power consumption for radar waveform and information rate utilizing various algorithms with: (a) $\delta_D = 0.55$, $r_{com} = 1.5$ npcu; (b) $\delta_D = 0.75$, $r_{com} = 2.0$ npcu; (c) $\delta_D = 0.95$, $r_{com} = 2.5$ npcu.

TABLE I
COMPARISON OF THE PROBABILITY OF DETECTION AND INFORMATION RATE UTILIZING DIFFERENT METHODS ($\delta_D = 0.95$, $r_{COM} = 2.5$ NPCU)

Indexes	Algorithms	$\overline{p_D}$	R_{com}(npcu)
[1]	The LPI-OPA scheme	0.95	2.5
[2]	The CBK-OPA scheme	1.0	2.5
[3]	Sub-optimal PA scheme	1.0	5.5287

transmitted to satisfy the requirements of both radar and communication subsystems. Hence, larger probability of detection and information rate implies that the constraints in problem (15) are more likely to be satisfied with a larger total power consumption.

Further, to verify the LPI performance improvement of the proposed LPI-OPA scheme, we define a parameter ρ namely the improvement of Schleher intercept factor

$$\rho = \frac{\alpha(\cdot) - \alpha_{\text{Sub-PA}}}{\alpha_{\text{Sub-PA}}} \times 100\% \qquad (33)$$

where $\alpha(\cdot)$ denotes the value of Schleher intercept factor by utilizing the specified algorithm, $\alpha_{\text{Sub-PA}}$ denotes the value of Schleher intercept factor by utilizing the suboptimal PA scheme. Schleher intercept factor is an important metric to evaluate the LPI performance of an active sensor, which is defined as [39]

$$\alpha_{\text{Schleher}} \triangleq \frac{R_I}{R_T} = \left(\frac{P_T G_T'^2 G_I^2 \lambda^2 S_T}{(4\pi) G_T G_R \sigma S_I^2} \right)^{\frac{1}{4}} \propto P_T^{\frac{1}{4}} \qquad (34)$$

where R_I denotes the maximum intercept range of passive interceptor, and R_T denotes the maximum detection range of active sensor, P_T is the peak transmitted power of the active sensor, G_T is the transmitting antenna gain, G_R is the receiving antenna gain, λ is the radar wavelength, σ is the target radar cross section, S_T is the sensitivity of the active sensor, G_T' is the active sensor's transmitting antenna gain in the direction of the interceptor, G_I is the receiving antenna gain of the interceptor, and S_I is the sensitivity of the interceptor. Specifically, if Schleher intercept factor is less than 1, the integrated system can fulfill its missions, whereas the intercept receiver cannot intercept its radiation. Otherwise, the transmission of integrated system can be intercepted by the interceptor. It is noteworthy that the smaller transmit power P_T is, the smaller Schleher intercept factor α_{Schleher} is. The definition in (33) also implies that the larger ρ is, the better LPI performance of the integrated multistatic radar and communication system is. This is due to the fact that the radiation strategy with smaller total power consumption will yield larger value of ρ, which means better LPI performance. In Fig. 9, the improvement of Schleher intercept factor for the LPI-OPA scheme and the CBK-OPA scheme is given for different probabilities of detection and information rates. From Fig. 9, it can be observed that the LPI-OPA scheme utilizes a small quantity of power resource to fulfill the requirements of both target detection and information transferring, and thus yields an enhanced LPI performance for the integrated multistatic radar and communication system.

Moreover, Table I compares the achieved probability of detection and information rate employing different algorithms. We take the probability of detection $\delta_D = 0.95$ and the desired threshold of information rate $r_{com} = 2.5$ npcu, respectively. As

minimizes the total radiated power for both radar waveforms and information signals while maintaining a specified target detection performance for the RR and a desired information rate for the CR. As is expected, the results in Fig. 8 show that the LPI-OPA scheme radiates the minimum power. To be specific, through the adequate assignment of the transmit power resource, our proposed scheme can save about 89% power dissipation for radar waveform when compared with the CBK-OPA in [15] and the suboptimal PA approach, and reduce the transmit power for information rate to 4.4% of that achieved by the suboptimal PA method. As aforementioned, with the increase of the probability of detection and information rate, the total transmitted power of the integrated system in the LPI-OPA scheme goes up. An intuitive explanation is that, as the probability of detection and information rate are increased, more power budget need to be
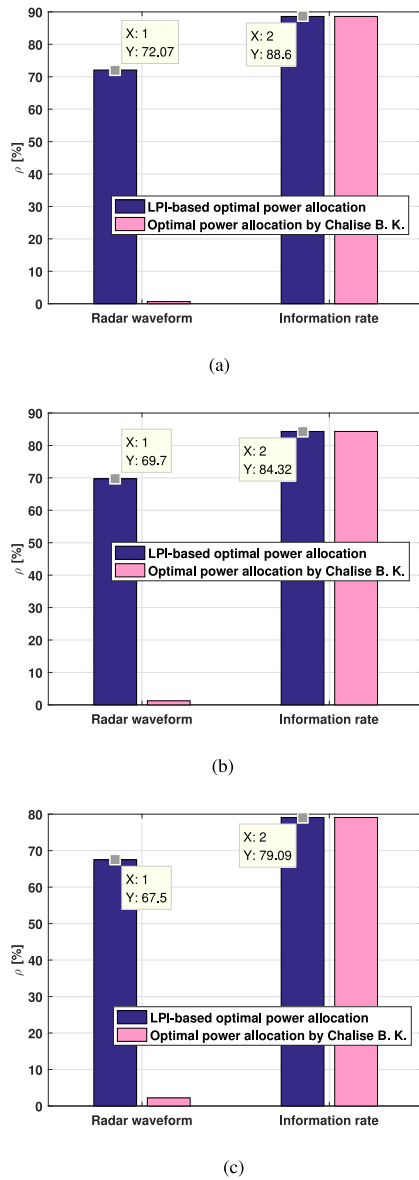
(a)

(b)

(c)

Fig. 9. Comparison of the improvement of Schleher intercept factor for the proposed LPI-OPA scheme and the CBK-OPA scheme with: (a) $\delta_D = 0.55$, $r_{com} = 1.5$ npcu; (b) $\delta_D = 0.75$, $r_{com} = 2.0$ npcu; (c) $\delta_D = 0.95$, $r_{com} = 2.5$ npcu.

it can be seen, the proposed LPI-OPA scheme can satisfy the requirements of both target detection and communication rate, where the threshold values of the probability of detection and information rate are achieved. Therefore, it is noteworthy that our LPI-OPA scheme outperforms other state of the art PA algorithms in terms of LPI performance, target detection performance, and information rate.

V. CONCLUSION

In this paper, we have investigated the LPI-OPA scheme for an integrated multistatic radar and communication system. The primary objective is to employ the optimization technique to minimize the total transmit power consumption for both target detection and information transferring, while satisfying a desired target detection performance for the RR and a specified

information rate for the CR. Since the probability of detection is not analytically tractable, its upper bound is derived. We analytically show that the resulting optimization problem can be reformulated as two subproblems, which can be solved by exploiting the technique of linear programming and the KKT conditions. The proposed LPI-OPA scheme has been evaluated via several numerical examples. More specifically, it is shown that the proposed LPI-OPA optimization scheme can offer unique advantage in terms of LPI performance enhancement compared to state-of-the-art PA algorithms.

The derivations show that the proposed LPI-OPA scheme can straightforwardly be generalized to the integrated distributed MIMO radar and communication system with multiple transmitters, multiple RRs, and multiple CRs. This will substantially expand the application scenarios of the study in this paper. A thorough investigation will be addressed in our future research.

REFERENCES

[1] B. Paul, A. R. Chiriyath, and D. W. Bliss, "Survey of RF communications and sensing convergence research," *IEEE Access*, vol. 5, pp. 252–270, 2017.

[2] C. G. Shi, F. Wang, M. Sellathurai, and J. J. Zhou, "Non-cooperative game theoretic power allocation strategy for distributed multiple-radar architecture in a spectrum sharing environment," *IEEE Access*, vol. 6, pp. 17787–17800, 2018.

[3] A. R. Chiriyath, B. Paul, G. M. Jacyna, and D. W. Bliss, "Inner bounds on performance of radar and communications co-existence," *IEEE Trans. Signal Process.*, vol. 64, no. 2, pp. 464–474, Jan. 2016.

[4] A. R. Chiriyath, B. Paul, and D. W. Bliss, "Radar-communications convergence: Coexistence, cooperation, and co-design," *IEEE Trans. Cogn. Commun. Netw.*, vol. 3, no. 1, pp. 1–12, Mar. 2017.

[5] B. Li and A. P. Petropulu, "Joint transmit designs for coexistence of MIMO wireless communications and sparse sensing radars in clutter," *IEEE Trans. Aerosp. Electron. Syst.*, vol. 53, no. 6, pp. 2846–2864, Dec. 2017.

[6] K. W. Huang, M. Bica, U. Mitra, and V. Koivunen, "Radar waveform design in spectrum sharing environment: Coexistence and cognition," in *Proc. IEEE Radar Conf. (RadarCon)*, 2015, pp. 1698–1703.

[7] M. Bica, K. W. Huang, V. Koivunen, and U. Mitra, "Mutual information based radar waveform design for joint radar and cellular communication systems," in *Proc. IEEE Int. Conf. Acoust., Speech Signal Process.*, 2016, pp. 3671–3675.

[8] M. Bica and V. Koivunen, "Generalized multicarrier radar: Models and performance," *IEEE Trans. Signal Process.*, vol. 64, no. 17, pp. 4389–4402, Sep. 2016.

[9] M. Bica and V. Koivunen, "Delay estimation method for coexisting radar and wireless communication systems," in *Proc. IEEE Radar Conf.*, 2017, pp. 1557–1561.

[10] C. G. Shi, F. Wang, M. Sellathurai, J. J. Zhou, and S. Salous, "Power minimization-based robust OFDM radar waveform design for radar and communication systems in coexistence," *IEEE Trans. Signal Process.*, vol. 66, no. 5, pp. 1316–1330, Mar. 2018.

[11] F. Liu, C. Masouros, A. Li, T. Ratnarajah, and J. M. Zhou, "MIMO radar and cellular coexistence: A power-efficient approach enabled by interference exploitation," *IEEE Trans. Signal Process.*, vol. 66, no. 14, pp. 3681–3695, Jul. 2018.

[12] B. K. Chalise, M. G. Amin, and B. Himed, "Performance tradeoff in a unified passive radar and communication system," *IEEE Signal Process. Lett.*, vol. 24, no. 9, pp. 1275–1279, Sep. 2017.

[13] Y. J. Liu, G. S. Liao, J. W. Xu, Z. W. Yang, and Y. H. Zhang, "Adaptive OFDM integrated radar and communications waveform design based on information theory," *IEEE Commun. Lett.*, vol. 21, no. 10, pp. 2174–2177, Oct. 2017.

[14] R. H. Xu, L. X. Peng, W. D. Zhao, and Z. C. Mi, "Radar mutual information and communication channel capacity of integrated radar-communication system using MIMO," *ICT Express*, vol. 1, pp. 102–105, 2015.

[15] B. K. Chalise, M. G. Amin, and B. Himed, "Performance tradeoff in a unified multi-static passive radar and communication system," in *Proc. IEEE Radar Conf.*, 2018, pp. 653–658.

[16] A. Deligiannis, A. Daniyan, S. Lambotharan, and J. A. Chambers, "Secrecy rate optimizations for MIMO communication radar," *IEEE Trans. Aerosp. Electron. Syst.*, vol. 54, no. 5, pp. 2481–2492, Oct. 2018, doi: 10.1109/TAES.2018.2820370.

[17] D. C. Schleher, "LPI radar: Fact or fiction," *IEEE Aerosp. Electron. Syst. Mag.*, vol. 21, no. 5, pp. 3–6, May 2006.

[18] C. W. Zhou, Y. J. Gu, S. B. He, and Z. G. Shi, "A robust and efficient algorithm for coprime array adaptive beamforming," *IEEE Trans. Veh. Technol.*, vol. 67, no. 2, pp. 1099–1112, Feb. 2018.

[19] Z. K. Zhang, S. Salous, H. L. Li, and Y. B. Tian, "Optimal coordination method of opportunistic array radars for multi-target-tracking-based radio frequency stealth in clutter," *Radio Sci.*, vol. 50, no. 11, pp. 1187–1196, 2016.

[20] J. K. Yan, W. Q. Pu, H. W. Liu, B. Jiu, and Z. Bao, "Robust chance constrained power allocation scheme for multiple target localization in colocated MIMO radar system," *IEEE Trans. Signal Process.*, vol. 66, no. 15, pp. 3946–3957, Aug. 2018.

[21] J. K. Yan, B. Jiu, H. W. Liu, B. Chen, and Z. Bao, "Prior knowledge based simultaneous multibeam power allocation algorithm for cognitive multiple targets tracking in clutter," *IEEE Trans. Signal Process.*, vol. 63, no. 2, pp. 512–527, Jan. 2015.

[22] J. K. Yan, H. W. Liu, B. Jiu, B. Chen, Z. Liu, and Z. Bao, "Simultaneous multibeam resource allocation scheme for multiple target tracking," *IEEE Trans. Signal Process.*, vol. 63, no. 12, pp. 3110–3122, Jun. 2015.

[23] J. K. Yan, H. W. Liu, W. Q. Pu, S. H. Zhou, Z. Liu, and Z. Bao, "Joint beam selection and power allocation for multiple target tracking in netted colocated MIMO radar system," *IEEE Trans. Signal Process.*, vol. 64, no. 24, pp. 6417–6427, Dec. 2016.

[24] Y. X. Lu, Z. S. He, Z. Y. Cheng, S. L. Liu, and X. Luo, "Adaptive resource allocation in decentralized colocated MIMO radar network for multiple targets tracking," in *Proc. IEEE Radar Conf.*, 2018, pp. 152–157.

[25] M. C. Xie, W. Yi, T. Kirubarajan, and L. J. Kong, "Joint node selection and power allocation strategy for multitarget tracking in decentralized radar networks," *IEEE Trans. Signal Process.*, vol. 66, no. 3, pp. 729–743, Feb. 2018.

[26] C. G. Shi, F. Wang, S. Salous, and J. J. Zhou, "Optimal power allocation strategy in a joint bistatic radar and communication system based on low probability of intercept," *Sensors*, vol. 17, 2017, Art. no. E2731, doi: 10.3390/s17122731.

[27] S. D. Blunt, P. Yatham, and J. Stiles, "Intrapulse radar-embedded communications," *IEEE Trans. Aerosp. Electron. Syst.*, vol. 46, no. 3, pp. 1185–1200, Jul. 2010.

[28] M. M. Bazaraa and C. M. Shetty, *Nonlinear Programming.* New York, NY, USA: Wiley, 1979.

[29] W. Karush, "Minima of functions of several variables with inequalities as side constraints," M.S. thesis, Dept. Math., Univ. Chicago, Chicago, IL, USA, 1939.

[30] M. Masjedi, M. Moddares-Hashemi, and S. Sadri, "Theoretical approach for target detection and interference cancellation in passive radars," *IET Radar, Sonar Navigat.*, vol. 7, no. 3, pp. 205–216, Mar. 2013.

[31] D. E. Hack, L. K. Patton, B. Himed, and M. A. Saville, "Detection in passive MIMO radar networks," *IEEE Trans. Signal Process.*, vol. 62, no. 11, pp. 2999–3012, Jun. 2014.

[32] B. K. Chalise and B. Himed, "GLRT detector in single frequency multistatic passive radar systems," *Signal Process.*, vol. 142, pp. 504–512, 2018.

[33] A. Deligiannis, A. Panoui, S. Lambotharan, and J. A. Chambers, "Game-theoretic power allocation and the Nash equilibrium analysis for a multistatic MIMO radar network," *IEEE Trans. Signal Process.*, vol. 65, no. 24, pp. 6397–6408, Dec. 2017.

[34] A. Kenarsari-Anhari and L. Lampe, "Power allocation for coded OFDM via linear programming," *IEEE Commun. Lett.*, vol. 13, no. 12, pp. 887–889, Dec. 2009.

[35] S. X. Yin and Z. W. Qu, "Resource allocation in multiuser OFDM systems with wireless information and power transfer," *IEEE Commun. Lett.*, vol. 20, no. 3, pp. 594–597, Mar. 2016.

[36] G. Alirezaei, O. Taghizadeh, and R. Mathar, "Optimum power allocation with sensitivity analysis for passive radar applications," *IEEE Sensors J.*, vol. 14, no. 11, pp. 3800–3809, Nov. 2014.

[37] S. P. Boyd and L. Vandenberghe, *Convex Optimization.* Cambridge, U.K.: Cambridge Univ. Press, 2004.

[38] C. G. Shi, F. Wang, M. Sellathurai, and J. J. Zhou, "Low probability of intercept based multicarrier radar jamming power allocation for joint radar and wireless communications systems," *IET Radar, Sonar Navigation*, vol. 11, no. 5, pp. 802–811, May 2017.

[39] C. G. Shi, J. J. Zhou, and F. Wang, "Low probability of intercept optimization for radar network based on mutual information," in *Proc. IEEE China Summit Int. Conf. Signal Inf. Process.*, 2014, pp. 683–687.

Chenguang Shi was born in Luoyang, China, 1989. He received the B.S. and Ph.D. degrees from the Nanjing University of Aeronautics and Astronautics (NUAA), Nanjing, China, in 2012 and 2017, respectively.

He is currently a Lecturer with the Key Laboratory of Radar Imaging and Microwave Photonics, NUAA, Ministry of Education. His main research interests include low probability of intercept optimization, radar network, adaptive radar waveform design, and target tracking.

Fei Wang received the M.S. degree and the Ph.D. degree from Jilin University, Changchun, China, in 2003 and 2006, respectively.

He is currently an Associate Professor with the Nanjing University of Aeronautics and Astronautics, Nanjing, China. His main research interests include aircraft radio frequency stealth, radar signal processing, and array signal processing.

Mathini Sellathurai (SM'06) is a Full Professor in signal processing and intelligent systems, Heriot-Watt University, Edinburgh, U.K. In her 15-year research on signal processing for communications, she has made seminal contributions on MIMO wireless systems. She has authored and coauthored 200 IEEE entries with 2300+ citations, given invited talks, and has written a book and several book chapters in topics related to this project.

Prof. Sellathurai was the recipient of the IEEE Communications Society Fred W. Ellersick Best Paper Award in 2005, Industry Canada Public Service Awards for contributions in science and technology in 2005, and Best Ph.D. Thesis Award (Silver Medal) from NSERC Canada in 2002. She is also a member for IEEE SPCOM Technical Strategy Committee, Editor for IEEE TRANSACTIONS ON SIGNAL PROCESSING (2009–2014, 2015-present). She is also the General Co-Chair of IEEE International Workshop on Signal Processing advances in Wireless Communications, 2016 in Edinburgh.

Jianjiang Zhou received the M.S. and the Ph.D. degrees from the Nanjing University of Aeronautics and Astronautics (NUAA), Nanjing, China, in 1988 and 2001, respectively.

He is currently a Professor and the Director of the Key Laboratory of Radar Imaging and Microwave Photonics, Ministry of Education, at NUAA. His main research interests include aircraft radio frequency stealth, radar signal processing, and array signal processing.

Sana Salous (SM'95) received the B.E.E. degree from the American University of Beirut, Beirut, Lebanon, in 1978, and the M.Sc. and Ph.D. degrees from Birmingham University, Birmingham, U.K., in 1979 and 1984, respectively.

She was an Assistant Professor with Yarmouk University, Irbid, Jordan, for four years. She was a Research Fellow with Liverpool University, Liverpool, U.K., for one year. She held a lectureship with the University of Manchester Institute of Science and Technology, Manchester, U.K., in 1989, where she was subsequently a Senior Lecturer and then a Reader. Since 2003, she has been the Chair in Communications Engineering with Durham University, Durham, U.K., where she is currently the Director of the Centre for Communication Systems. Her current research interests include radio channel characterization in various frequency bands ranging from skywave in the HF band to millimeter bands at 60 GHz, the design of radar waveforms, and novel radio channel sounders, and radar systems for radio imaging.

Dr. Salous is a Fellow of the Institution of Engineering and Technology. She is the Chair of the Commission C on Radio Communication and Signal Processing Systems of the International Union of Radio Science. She is an Associate Editor of the *Radio Science* journal.